# Local Environment Effects in the Vibrational Properties of Disordered Alloys: an Embedded-Atom Method Study of $Ni_3Al$ and $Cu_3Au$

*D. Morgan, J.D. Althoff, and D. de Fontaine*
*Department of Materials Science and Mineral Engineering*
*University of California, Berkeley, CA 94720*

*(Submitted 27 January 1998; in revised form 8 June 1998)*

**Local environment effects are important for providing a framework for understanding the changes in vibrational properties that result from disordering. In the present work the effects of local environments on thermodynamic quantities are examined using the embedded-atom method (EAM) for $Ni_3Al$ and $Cu_3Au$. Projections of the density of states onto different local environments are performed, and a local cluster expansion is calculated. It is found that the contribution to the entropy from a given atom is primarily determined by the atom and its first few neighbor shells. Relaxations are seen to qualitatively change the dependence of the entropy on local environment, changing the sign of the dominant interactions. Also, relaxations are found to extend the range of point and pair interactions and to increase the importance of multisite interactions. These results suggest that a special quasi-random structure (SQS), a small supercell constructed to approximate the local environments of the disordered phase, might be able to reproduce the disordered phase vibrational thermodynamics. It is found that an eight-atom SQS can accurately represent the vibrational thermodynamic properties of the disordered phase, implying that it could be a powerful tool for first-principles vibrational studies.**

## 1. Introduction

The influence of vibrational effects on phase stability is at present poorly understood. Until recently most phase diagram calculations were performed without including vibrational contributions, which were assumed to be small. Now evidence is emerging that vibrations may play an important part in determining phase diagrams. Recent experimental work on $Ni_3Al$ (Ref 1, 2) and $Cu_3Au$ (Ref 3) suggests that the vibrational entropy difference ($\Delta S$) between the disordered and $L1_2$ phases is quite significant compared with the configurational effects. Theoretical calculations on these systems have also suggested that the vibrational $\Delta S$ could be quite large (Ref 4-7), although recent first-principles calculations have obtained a small vibrational $\Delta S$ for $Ni_3Al$ (Ref 8). The excitement and controversy these experimental and theoretical results have produced make clear the need for further study.

In this work, the embedded-atom method (EAM) (Ref 9, 10), coupled with the quasi-harmonic method (Ref 11, 12), is used to study vibrational properties of $Ni_3Al$ and $Cu_3Au$. The vibrational $\Delta S$ is calculated both with and without local relaxation, obtaining reasonable agreement with experimental values for $Ni_3Al$ but not for $Cu_3Au$. The effects of relaxation on the vibrational $\Delta S$ are found to be fairly small for $Ni_3Al$, while for $Cu_3Au$ the relaxations have an important qualitative effect.

The influence of local environment is studied in some detail. Projections of the density of states onto different local environments are determined and used to calculate the local entropy. A cluster expansion (Ref 13-16) of the local entropy is performed in order to analyze the important aspects of the chemical environment. It is found that the contribution to the entropy from a given atom is primarily determined by the atom and its first few neighbor shells. Relaxations are seen to qualitatively change the dependence on local environment, changing the sign of the dominant interactions. Also, relaxations are found to extend the range of point and pair interactions and increase the importance of multisite interactions.

The results of the cluster expansion suggest that special quasi-random structures (SQSs) (Ref 17-19) might be used successfully to model the vibrational thermodynamic properties of the disordered phase. By comparing with results from a large (256-atom) disordered supercell, it is found that an eight-atom (SQS-8) can accurately represent the vibrational thermodynamic properties of the disordered phase. This suggests that the SQS-8 could be a powerful tool for first-principles vibrational studies. Including relaxation causes the SQS-8 to give a less accurate representation of the disordered phase vibrational thermodynamics. This can be understood in terms of the longer-range and multisite interactions found to be important in the relaxed cluster expansion.

This article is arranged as follows. The following section, section 2, is a description of the computational methods, including the EAM, the quasi-harmonic method, the calculation of local thermodynamic quantities, the cluster expansion as applied to local quantities, and the SQS. Section 3 gives the results of the cluster expansion of the local entropy for both the locally unrelaxed and relaxed cases. Section 4 compares the results of vibrational thermodynamic properties calculated

with the SQS-8 and a large (256-atom) disordered supercell. Section 5 gives a summary of the results and the conclusions.

## 2. Computational Methods

### 2.1 Embedded-Atom Method

A detailed discussion of the EAM is given in Ref 10 and is discussed only briefly here. The EAM is a semiempirical many-body potential, the parameters of which are fit to experimental or first-principles data. The $Ni_3Al$ potentials being used were developed by Voter and Chen (Ref 20), and their applicability to the calculation of vibrational thermodynamic properties has been shown in Ref 6. The $Cu_3Au$ potentials were developed by Foiles et al. in the context of developing a set of potentials for a number of transition metals (Ref 21). Unlike the $Ni_3Al$ potentials, the $Cu_3Au$ potentials were fit using only pure-element properties and dilute heats of solution. Therefore, they may not be as reliable when used for alloy properties; for example, it is well known that these potentials get the incorrect sign for the $L1_2/D0_{22}$ energy difference in $Cu_3Au$. Preliminary results suggest that these $Cu_3Au$ potentials give a reasonable representation of the $L1_2$ vibrational spectrum and thermal expansion, but further testing of the potentials is required to determine their accuracy for quantitative vibrational thermodynamic calculations. Although the EAM is always somewhat suspect because of the approximate nature of the potential, it allows one to perform calculations on systems more than 100 times the size that would be accessible to more accurate first-principles calculations. Because the EAM almost certainly provides a reasonable physical model for the alloy, it is appropriate to use it for the tests of the SQS and qualitative trends that are the focus of this article.

### 2.2 Quasi-Harmonic Method

The quasi-harmonic method is discussed in Ref 11. It is a simple extension of the harmonic approach, discussed in Ref 11 and 12, to approximately include anharmonic effects. In the harmonic approximation, the vibrations are treated only to second order in the displacements. The dynamical matrix is then diagonalized to find eigenvectors and eigenvalues, which in turn can be used to calculate densities of states and thermodynamic properties. For example, in the harmonic approximation, the entropy can be found from the density of states by the formula:

$$S(T) = k_B \int d\omega g(\omega)\left|(x/2)/\tanh(x/2) - \log[2\sinh(x/2)]\right| \quad \text{(Eq 1)}$$

where $T$ is the temperature, $g(\omega)$ is the density of states, $x = \hbar\omega/k_BT$, and the integral is for all positive $\omega$. In the quasi-harmonic approach, the harmonically determined frequencies are considered as function of volume. The vibrational free energy can then be found as a function of volume, and by minimizing the free energy to find the equilibrium volume, the thermal expansion effects are approximately included. The quasi-harmonic results have been compared with those of more accurate Monte Carlo calculations for $Ni_3Al$, and it was found that the quasi-harmonic method significantly overestimates the thermal expansion, especially at high temperature. However, the effects have no qualitative impact, as using the Monte Carlo equilibrium volumes (rather than those from the quasi-harmonic method) changes the vibrational $\Delta S$ by only about 25%. Careful testing of the quasi-harmonic approximation compared to Monte Carlo results can be found in Ref 22.

### 2.3 Local Thermodynamic Quantities

In the harmonic approximation, thermodynamic quantities can be calculated by straightforward integration of the vibrational density of states (DOS) weighted by the appropriate function. Local thermodynamic quantities can be calculated in a similar manner using the projected or local DOS.

This article defines a projected DOS in the following manner. The DOS can be expressed as a trace over a Green's function (Ref 11) as:

$$D(\omega) = -\frac{2\omega}{\pi}\,\mathrm{Im}\,\mathrm{Tr}\,\hat{G}(\omega) \quad \text{(Eq 2)}$$

with:

$$\hat{G}(\omega, \vec{k}) = (\omega^2\,\hat{1} - \hat{D}(\vec{k}) + i\varepsilon)^{-1} \quad \text{(Eq 3)}$$

Here Tr means the trace, Im means take the imaginary part, and $\hat{D}$ is the dynamical matrix, $\hat{1}$ is a unit matrix of appropriate size, and $\varepsilon \rightarrow 0^+$. The trace may be taken in any basis; for example, taking the trace in the basis of phonon eigenvectors $|\Psi_i\rangle$ leads to the standard expression for the DOS:

$$D(\omega) = \sum_i \delta(\omega - \omega_i) \quad \text{(Eq 4)}$$

Consider now a basis $|m, \mu\rangle$ where $m$ labels the atoms and $\mu$ labels the Cartesian component; each of the members of the basis is a vector of length $3N$ ($N$ is the number of atoms in the unit cell) with a single element equal to one (the one corresponding to atom $m$ and Cartesian direction $\mu$) and all other elements zero. By evaluating the trace in this basis and making use of the closure property of the eigenvectors one obtains:

$$D(\omega) = \sum_{m,\mu}\sum_i |\langle m,\mu|\Psi_i\rangle|^2\,\delta(\omega - \omega_i) = \sum_{m,\mu} D_{m,\mu}(\omega) \quad \text{(Eq 5)}$$

The inner product $|\langle m,\mu|\Psi_i\rangle|$ is simply the Cartesian component $u$ of the amplitude of displacement of atom $m$ in mode $i$. The quantity $D_{m,\mu}(\omega)$ is the density of states projected onto atom $m$ and direction $\mu$. Equation 5 may be used to generate a variety of different projected DOSs. In this work the DOS is projected onto a given atom, which is done by constructing the sum of $D_{m,\mu}(\omega)$ over all $\mu$ for the given atom $m$.

The total DOS can be written as a sum of the projected DOS for each atom. Therefore, any thermodynamic quantity calculated by integrating over the total DOS can be written as a sum of terms each involving integrals over the projected DOS for each atom. These terms can be considered the local contribu-

tion from each atom to the total thermodynamic quantity. Studying the influence of the surrounding environment on the thermodynamic contribution of a given atom provides insight into how local environments affect the total alloy thermodynamics.

### 2.4 Cluster Expansion

In order to make a quantitative analysis of the influence of the local environment, a cluster expansion (CE) of the local thermodynamics is performed. The CE formalism is generally appropriate for modeling the dependence of a quantity on chemical disorder (Ref 13, 14). The CE is usually applied to formation energies, although recently it has been extended to the study of vibrational properties (Ref 8, 15, 16). The idea of fitting interactions to represent local vibrational properties has also been pursued previously (Ref 23), but it was not done within the modern CE formalism, and only first-neighbor environments were included.

The CE of a local function is slightly different from the CE of a global function, so it will be discussed in some detail here. The CE formalism allows any function of configuration (the occupation of each lattice site) to be written in a generalized Ising form. In the CE formalism for an *A-B* binary alloy, the alloy configuration is represented by pseudospin variables, defined as:

$$\sigma(p) = -1 \text{ when an atom of type } A \text{ is on site } p \quad \text{(Eq 6a)}$$

$$\sigma(p) = +1 \text{ when an atom of type } B \text{ is on site } p \quad \text{(Eq 6b)}$$

Any function of configuration $F$ can be written:

$$F(\sigma) = \sum_{\alpha} V_{\alpha}\Phi_{\alpha}(\sigma) \quad \text{(Eq 7)}$$

where $\sigma$ denotes the pseudospin configuration of the whole lattice, $\alpha$ denotes a cluster of sites on the lattice, and $N$ is the number of lattice sites. The sum is over all possible clusters. $\Phi_{\alpha}$ is called a cluster function and is equal to the product of the pseudospin values on all the sites in cluster $\alpha$. The $V_{\alpha}$ are the effective cluster interactions (ECI) and represent how the atoms interact (Ref 14). The ECI are defined by the projection:

$$V_{\alpha} = \langle F(\sigma)\Phi_{\alpha}(\sigma)\rangle = \frac{1}{2^N}\sum_{\sigma} F(\sigma)\,\Phi_{\alpha}(\sigma) \quad \text{(Eq 8)}$$

where the summation is over all possible configurations of the system.

The symmetry of the parent lattice on which the cluster expansion is performed reduces the number of independent ECI. Let $S$ be a symmetry operation of the parent lattice. For a global quantity, $F(\sigma)$, it is true that:

$$F(\sigma) = F(S(\sigma)) \quad \text{(Eq 9)}$$

and this can be used to show that:

$$V_{\alpha} = V_{S(\alpha)} \quad \text{(Eq 10)}$$

For a local quantity, $F^p(\sigma)$, which depends on configuration and which lattice site, $p$, is being considered, it is only true that:

$$F^p(\sigma) = F^{S(p)}(S(\sigma)) \quad \text{(Eq 11)}$$

Equation 11 shows only that the equality in Eq 10 holds when $p = S(p)$. This follows from the fact that:

$$\begin{aligned} V_{\alpha} &= \frac{1}{2^N}\sum_{\sigma} F^p(\sigma)\Phi_{\alpha}(\sigma) \\ &= \frac{1}{2^N}\sum_{\sigma} F^p(S^{-1}(\sigma))\,\Phi_{\alpha}(S^{-1}(\sigma)) \\ &= \frac{1}{2^N}\sum_{\sigma} F^{S(p)}(\sigma)\Phi_{S(\alpha)}(\sigma) \\ &= \frac{1}{2^N}\sum_{\sigma} F^p(\sigma)\Phi_{S(\alpha)}(\sigma) \\ &= V_{S(\alpha)} \end{aligned} \quad \text{(Eq 12)}$$

Therefore Eq 10 is true by symmetry only when $S$ is both a symmetry operation of the parent lattice and when $p = S(p)$; that is, $S$ is an element of the parent lattice point group for the point $p$.

A common method of determining the ECI is the Connolly-Williams, or structure inversion, method (Ref 14, 24-27) (SIM). This involves choosing a set of clusters whose corresponding ECI are expected to be the most significant. Reasonable criteria for establishing whether a cluster is likely to have a significant corresponding interaction are:

- The cluster has as few points as possible.
- The cluster is as compact as possible.
- For a local CE, the cluster contains the relevant local point $p$.

These criteria are fairly standard except for the last one, which needs to be added for the case of a local CE. Following these criteria, only point and pair ECI are used in this article.

Using the SIM with the usual CE formalism involves calculating the quantity of interest for a number of different lattice configurations to get independent values to which one can fit ECI. In the case of a local quantity, a number of different values and local environments can be obtained from a single unit cell, particularly if it is large and disordered. For the authors' calculations, a large number of distinct local values and environments are obtained for fitting using a single 256-atom disordered unit cell.

### 2.5 Special Quasi-Random Structures

The special quasi-random structures (SQSs) (Ref 17-19) are small unit cell lattice configurations that approximate the local environments of the disordered phase. This is done by

constructing the SQS to reproduce as closely as possible the short-range correlations of the disordered phase. The SQSs are very useful for first-principles calculations, as they allow one to directly calculate disordered phase properties using a tractable number of atoms. They have been shown previously to represent accurately such properties as total energies and band gaps (Ref 19), but they have not previously been tested on vibrational properties to the knowledge of the authors. Here, SQS-8 is the focus because it is the smallest unit cell that can give a reasonable representation of the disordered phase. Larger unit cells are of less interest at this point as eight atoms is already pushing the computational limits of present first-principles phonon methods.

The primitive lattice vectors, basis atom locations, and short-range correlations of the SQS-8 used in this work (Ref 28) are given in Tables 1 to 3, respectively. The correlations of the random disordered state are also included for comparison. It can be seen that this SQS-8 reproduces the first three neighbor pair correlations of the random disordered state almost perfectly, but that for farther pairs the agreement gets worse. The triplet correlations are also quite good, but the tetrahedron correlation shows significant deviation from the disordered state.

## 3. Cluster Expansion Results

A local CE of the local entropy ($S^p$) has been performed as described in section 2.4. $S^p$ was found by integrating the DOS projected onto site $p$ (the projected DOS is normalized to 3) against the appropriate function (see section 2.3). $S^p$ was found for each site $p$ of a large disordered cell of 256 atoms, and checks were made for a 500-atom cell to assure that results were converged with respect to size. The calculations were performed at a lattice parameter of 3.614 Å (for $Ni_3Al$) and 3.76 Å (for $Cu_3Au$), and a temperature of 600 K. The calculations are converged to within about 0.01 $k_B$ with respect to the $k$-point sampling used to calculate the DOS. The SIM was then used to fit ECI to $S^p$. A large number of ECI can be determined from a single disordered cell because it contains a large number of distinct local entropies and environments. The ECI considered corresponds to the zero cluster, the point cluster $p$, and, for each point $p'$ in the first eight nearest-neighbor (nn) shells,

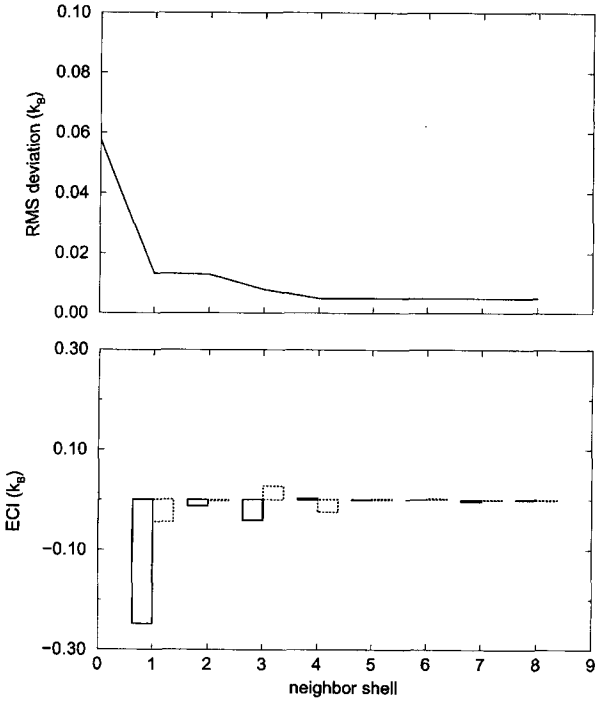


**Fig. 1** Unrelaxed $Ni_3Al$. The RMS error in the cluster expansion of the local entropy and the point (solid) and pair (dashed) effective cluster interactions themselves.

**Table 1 Primitive Lattice Vectors (PLV), in Units of Lattice Parameter**

| PLV | X | Y | Z |
|---|---|---|---|
| PLV I | 1 | 0 | 0 |
| PLV II | 0.5 | 1 | 0.5 |
| PLV III | –0.5 | –1 | 1.5 |

**Table 2 Basis Atom Locations, in Units of the Primitive Lattice Vectors**

| Atom type | PLV I | PLV II | PLV III |
|---|---|---|---|
| *A* | 0.5 | –0.25 | 1.25 |
| | 0.5 | 0.25 | 0.75 |
| | 1 | 0.75 | 0.75 |
| | 0 | –0.75 | 1.25 |
| | 1 | 0.25 | 0.25 |
| | 0 | –0.25 | 1.75 |
| *B* | 1 | 0.25 | 1.25 |
| | 0 | –0.25 | 0.75 |

**Table 3 Correlations, Lattice Averaged Cluster Functions**

| Cluster type | Vertices | SQS-8 | Random disordered state |
|---|---|---|---|
| Points | (000) | -½ | -½ |
| Pairs | | | |
| 1 neighbor | (000),(110) | ¼ | ¼ |
| 2 neighbor | (000),(200) | ⅓ | ¼ |
| 3 neighbor | (000),(112) | ¼ | ¼ |
| 4 neighbor | (000),(022) | 0 | ¼ |
| 5 neighbor | (000),(013) | ⅙ | ¼ |
| 6 neighbor | (000),(222) | 0 | ¼ |
| 7 neighbor | (000),(123) | ⅓ | ¼ |
| 8 neighbor | (000),(004) | ⅔ | ¼ |
| Triplets | | | |
| 1 neighbor | (000),(110),(101) | -¼ | -⅛ |
| 2 neighbor | (000),(110),(200) | -⅙ | -⅛ |
| Quadruplets | | | |
| 1 neighbor | (000),(110),(101),(011) | ½ | 1/16 |

the point $p'$ and pair $pp'$ clusters. Cluster expansions were performed for both locally unrelaxed and locally relaxed configurations. The results for locally unrelaxed $Ni_3Al$, locally relaxed $Ni_3Al$, locally unrelaxed $Cu_3Au$, and locally relaxed $Cu_3Au$ are given in Fig. 1 to 4, respectively. The top halves of these figures show the RMS error in the values predicted by the ECI compared with the exact calculated values. The RMS errors are plotted as a function of the number of neighbor shells included in the CE. In the bottom half of these figures the point (solid) and pair (dashed) ECI themselves are plotted for each neighbor shell.

In the unrelaxed case, the local environment is strongly dominated by the first-neighbor shell for both alloys, although most strikingly for $Cu_3Au$. This can be seen by the sharp drop in the RMS error after the first shell and by the larger values of the first shell ECI. In both alloys the ECI are essentially zero after the fourth-neighbor shell, and in both alloys the inclusion of ECI out to the fourth-neighbor shell brings the RMS error down to about 0.01 $k_B$, which shows that multisite interactions are not important.

When local relaxation is included, there are a number of important effects. First, for both alloys the ECI become longer range, as clearly evidenced by significant fifth-neighbor shell ECI. Second, in both alloys the RMS error decreases only to around 0.03 $k_B$, not nearly as low a value as was obtained in the unrelaxed case. This is probably due to an increase in the importance of multisite interactions. It is unlikely that the RMS error is large due to a failure to include enough pairs, because ECI out near the eighth-neighbor shell do not seem to be significantly improving the RMS error. Finally, there is a dramatic change of sign of the dominant first-neighbor shell ECI when local relaxation is included. This implies that the dependence on local environment is qualitatively different between the unrelaxed and relaxed case.

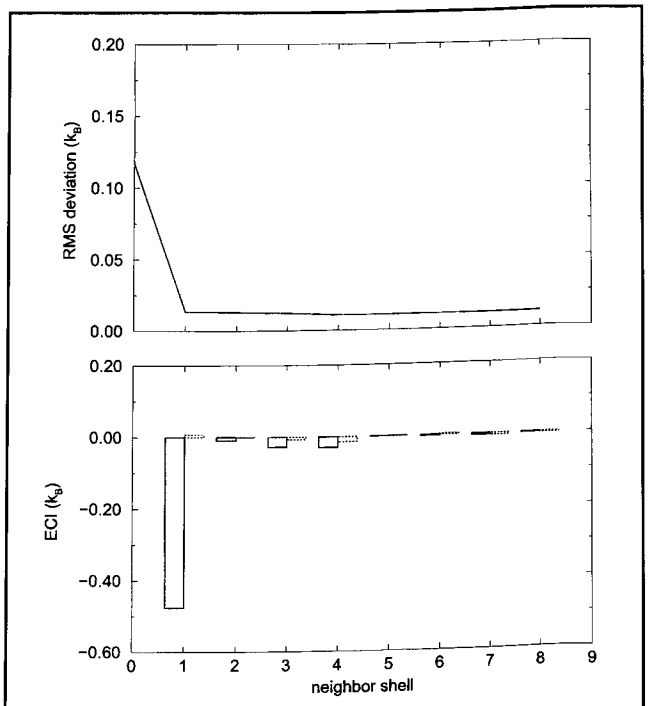


**Fig. 3** Unrelaxed $Cu_3Au$. The RMS error in the cluster expansion of the local entropy and the point (solid) and pair (dashed) effective cluster interactions themselves.

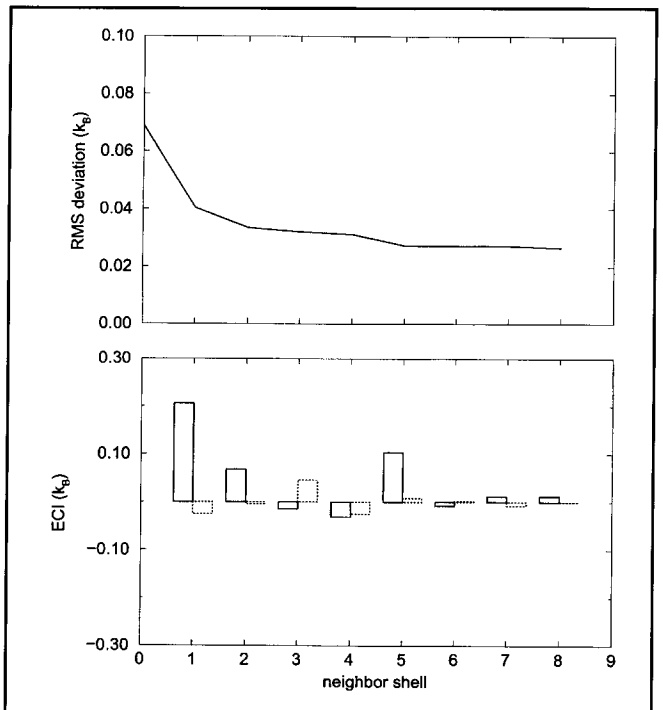


**Fig. 2** Relaxed $Ni_3Al$. The RMS error in the cluster expansion of the local entropy and the point (solid) and pair (dashed) effective cluster interactions themselves.

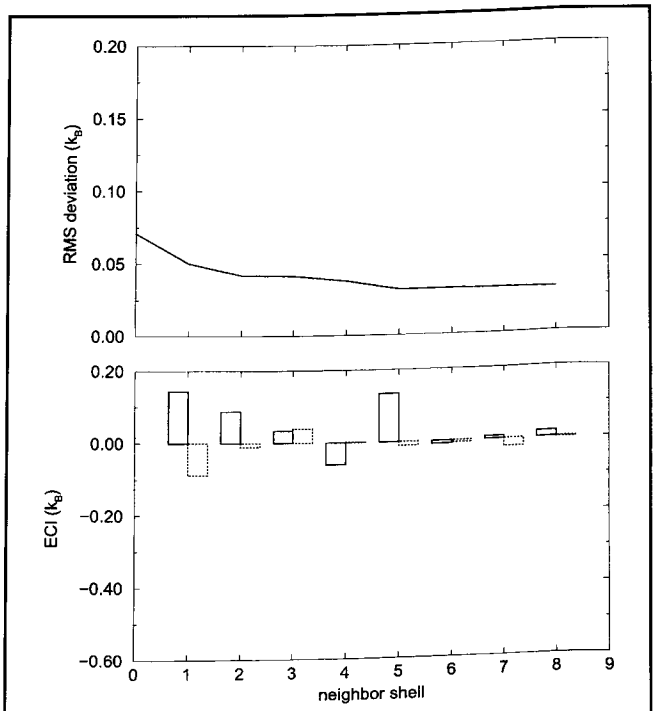


**Fig. 4** Relaxed $Cu_3Au$. The RMS error in the cluster expansion of the local entropy and the point (solid) and pair (dashed) effective cluster interactions themselves.

The qualitative effect of relaxation can be seen more plainly in Fig. 5 and 6 for $Ni_3Al$ and $Cu_3Au$, respectively. In these figures, the local entropy has been plotted as a function of the nearest-neighbor shell point correlation function for both the relaxed (X) and unrelaxed (open circle) cases. The first thing to notice about these figures is that the local entropies are quite distinct for the two types of atoms. This is a simple mass effect, and in both cases the heavier atoms, which have lower frequency modes, have the higher local entropy. However, relaxation also has a profound effect. For the unrelaxed case in both alloys, the local entropy on an atom is seen to decrease as its nearest-neighbor environment becomes more *B*-atom (Au or Al) rich. For the locally relaxed case just the opposite occurs, and the local entropy on an atom is seen to increase as its nearest-neighbor environment becomes more *B*-atom rich. The change of slope is what accounts for the change of sign in the dominant first-shell ECI with the inclusion of relaxation. The relaxation effect can be simply understood in terms of size mismatch. Both Cu-Au and Ni-Al have a very large size mismatch between their constituents, the *B*-type atom (Au or Al) being the larger in both cases. Therefore, in the unrelaxed alloy, the addition of large *B* atoms to the local environment will create more crowding, higher electron densities, and stronger force constants, which will lead to a decrease in the local entropy. However, in the relaxed alloy, the addition of large *B* atoms to the local environment will cause atoms to be pushed away, lowering the electron density and decreasing the force constants; this will lead to an increase in the local entropy. The effect of size on local environment for the unrelaxed and relaxed cases is shown in Fig. 7.

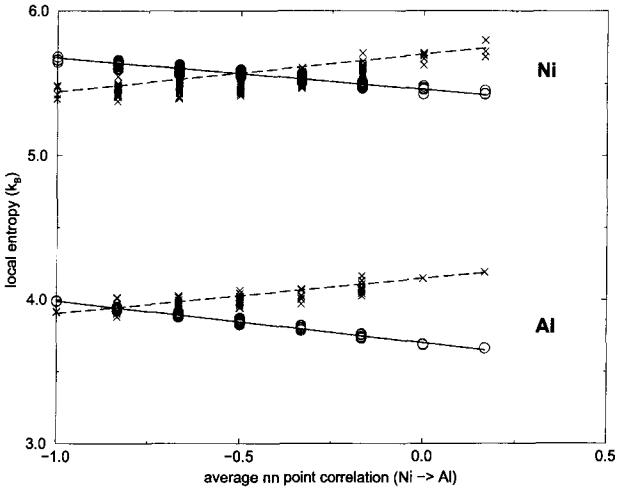


**Fig. 5** $Ni_3Al$. The local entropy as a function of the nearest-neighbor point correlation for both the locally unrelaxed (open circle) and locally relaxed (X) cases. Lines are drawn to assist the eye.

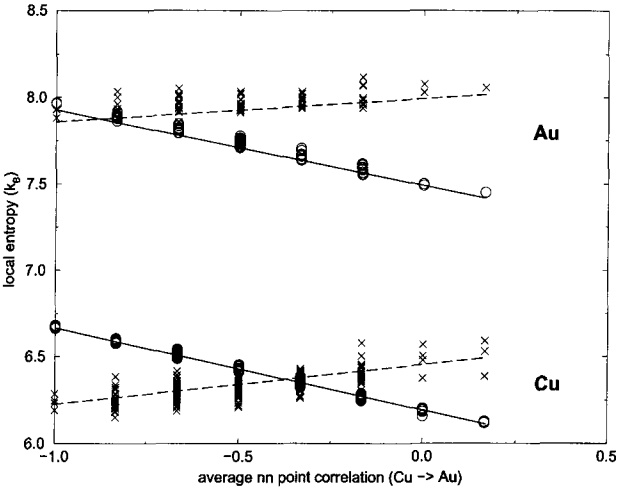


**Fig. 6** $Cu_3Au$. The local entropy as a function of the nearest-neighbor point correlation for both the locally unrelaxed (open circle) and locally relaxed (X) cases. Lines are drawn to assist the eye.

The reasonably short-range influence of the local environment suggests that a small unit cell with local environments similar to the disordered phase might be able to accurately model its vibrational properties.

## 4. Special Quasi-Random Structure Results

A comparison is made between an eight-atom special quasi-random structure (SQS-8) and a randomly decorated 256-atom supercell. The details of the SQS are discussed in section 2.5. The calculations are done in the quasi-harmonic approximation (see section 2.2) and are well converged with respect to *k*-point sampling and system size (for the disordered phase). Details of this implementation of the quasi-harmonic

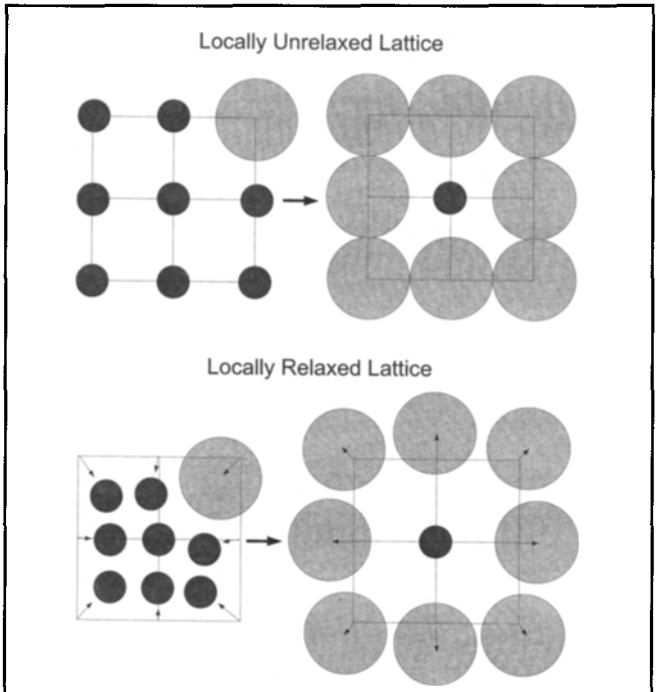


**Fig. 7** The effects of adding large atoms to the local environment. In the unrelaxed case, the crowding decreases the local entropy. In the relaxed case, the spreading increases the local entropy.

method can be found in Ref 6. Comparisons are given for the entropy difference ($\Delta S$) between the structure being considered (SQS-8 or 256-atom cell) and the $L1_2$ structure. The values of $\Delta S$ as a function of temperature are given for the 256-atom supercell (solid line) and the SQS-8 (dashed line) for locally unrelaxed $Ni_3Al$, locally relaxed $Ni_3Al$, locally unrelaxed $Cu_3Au$, and locally relaxed $Cu_3Au$, in Fig. 8 to 11, respectively. No cell external relaxations (e.g., *c/a* relaxation) are included in either the disordered phase or the SQS-8.

First, consider the values of $\Delta S$ that were obtained. The predictions for $\Delta S$ for these $Ni_3Al$ potentials (Ref 20) have been found previously within the quasi-harmonic approximation (Ref 6). For $Ni_3Al$ the value of $\Delta S$ is in good agreement with the experiments (Ref 1, 2), although the influence of thermal expansion on the theoretical results is quite significant, while it plays a small role in the experiments. Also, the experimentally measured lattice parameter of the disordered phase samples for which $\Delta S$ was measured seems to be smaller than that of the $L1_2$ phase (Ref 7), which is in strong disagreement with other theoretical (Ref 6, 8, 29, 30) and experimental (Ref 31) results, including those obtained here. A complete understanding of the roles of grain size, lattice parameter, and thermal expansion in the experiments and calculations performed on this system has not yet been obtained, and the issues are presently being investigated.

For $Cu_3Au$ the unrelaxed value of $\Delta S$ is in good agreement with previous experimental (Ref 3) and theoretical (Ref 4, 5) work, but when local relaxations are included, the value of $\Delta S$ drops essentially to zero. This disagreement may be due to problems in the $Cu_3Au$ EAM potential being used (see section 2.1), and attempts are presently underway to generate a more accurate potential based on alloy data. Even if the potentials

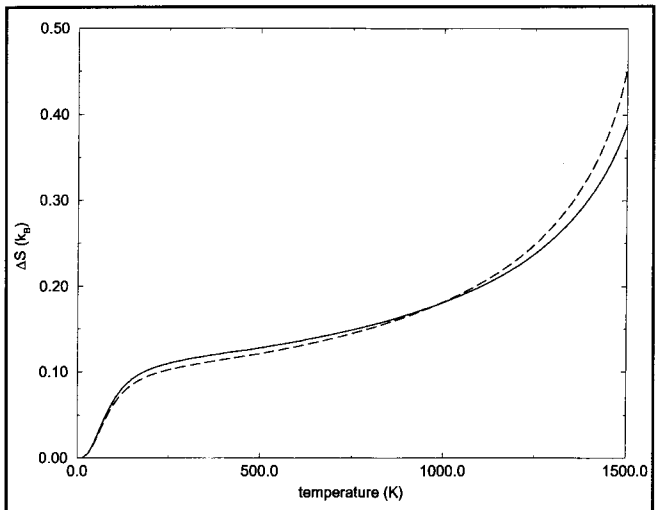


**Fig. 8** Unrelaxed $Ni_3Al$. The entropy difference with respect to the $L1_2$ phase for a disordered 256-atom cell (solid line) and an SQS-8 (dashed line).

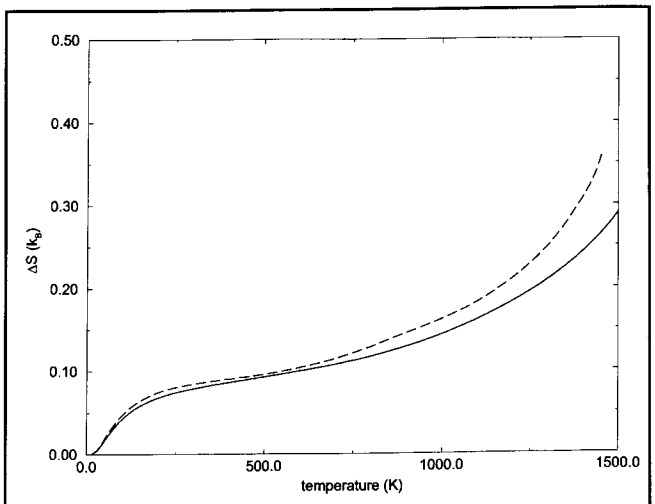


**Fig. 9** Relaxed $Ni_3Al$. The entropy difference with respect to the $L1_2$ phase for a disordered 256-atom cell (solid line) and an SQS-8 (dashed line).

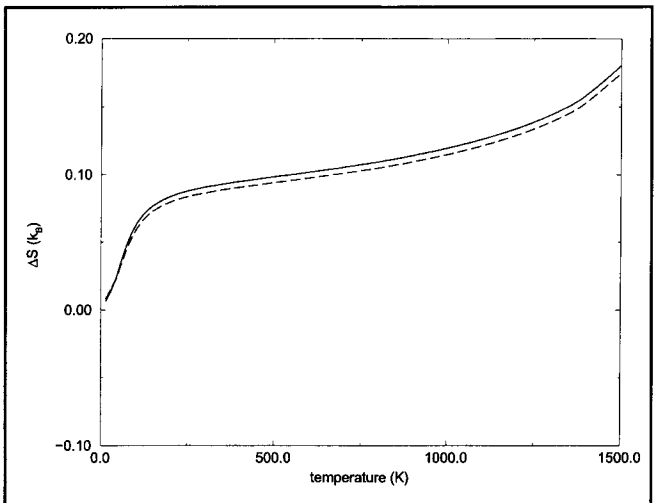


**Fig. 10** Unrelaxed $Cu_3Au$. The entropy difference with respect to the $L1_2$ phase for a disordered 256-atom cell (solid line) and an SQS-8 (dashed line).

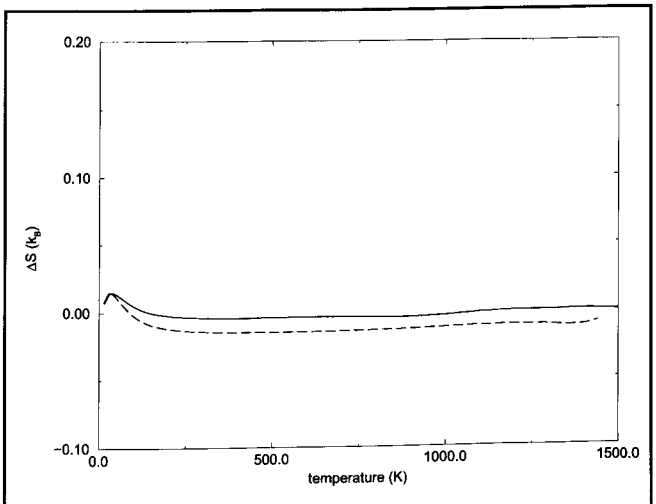


**Fig. 11** Relaxed $Cu_3Au$. The entropy difference with respect to the $L1_2$ phase for a disordered 256-atom cell (solid line) and an SQS-8 (dashed line).

are somewhat inaccurate for $Cu_3Au$, viewed as a realistic model system they demonstrate how large an impact local relaxations can have on the vibrational thermodynamics.

For both alloys the agreement between the SQS-8 and the 256-atom supercell is quite good. It is somewhat worse for $Ni_3Al$, particularly at very high temperatures, but still within a few tenths of a $k_B$ on average. This is to be expected from the previous results, as the SQS-8 only models the short-range correlations of the disordered phase accurately, and the interactions for $Ni_3Al$ are somewhat longer range than for $Cu_3Au$. For both alloys, the agreement becomes slightly worse when local interactions are included. Again, this is to be expected because the interactions become longer range when relaxations are included.

There are some aspects of the approach taken here that may overestimate the accuracy of the SQS-8 for calculating vibrational thermodynamic properties. The first is that the EAM often produces force constants that are somewhat shorter range than those found from first-principles or experiment. Because the SQS-8 models longer-range correlations less effectively, this would bias the above results in its favor. In addition, for the systems studied here with the EAM, the large values of $\Delta S$ are due primarily to volume effects. When a large $\Delta S$ is obtained, it is primarily due to the larger value of the disordered phase volume. If the calculations were performed at a fixed volume, all the high temperature values of $\Delta S$ would be within about 0.03 $k_B$ of zero. Because effects based on the overall volume are presumably less sensitive to the exact correlations than those based on subtle rearrangements of the vibrational modes, the SQS-8 may not provide as accurate a model for the vibrational properties of the disordered phase as the above calculations suggest for systems based on subtle rearrangements of the vibrational modes.

A conservative error estimate for $\Delta S$ is about 0.03 $k_B$ from these calculations. This is significantly below the values of around 0.1 to 0.4 $k_B$ that previous experiments and theoretical calculations have found in these alloys, and it would therefore be an acceptable error for many first-principles calculations. Even with the caveats mentioned above, the small errors found strongly suggest that the SQSs are a powerful tool for first-principles vibrational studies.

## 5. Summary and Conclusions

The authors have performed a study of local environment effects on vibrational thermodynamic properties using the embedded-atom method and the quasi-harmonic method for $Ni_3Al$ and $Cu_3Au$. The local entropies on all atoms in a large disordered cell were calculated using projections of the density of states onto each atom. These local entropies were then studied using a local cluster expansion formalism. By observing the effective cluster interactions, it was shown that the contribution to the entropy from a given atom is primarily determined by the atom and its first few neighbor shells. The role of local relaxations were also investigated. It was found that local relaxations can completely change the dependence on local environment, actually changing the sign of the dominant interactions. This effect was explained qualitatively in terms of the size mismatch of the constituent atoms. Also, local relaxations were found to extend the range of point and pair interactions and increase the importance of multisite interactions.

These results suggested that a special quasi-random structure (SQS), a small supercell constructed to approximate the local environments of the disordered phase, might be able to reproduce the disordered phase vibrational thermodynamics. The use of SQSs for vibrational properties had not previously been tested to the knowledge of the authors. It was found that an eight-atom SQS can accurately represent the vibrational thermodynamic properties of the disordered phase (modeled by a randomly decorated 256-atom cell). These results suggest that SQSs will be a powerful tool for first-principles vibrational studies.

The entropy difference between the disordered and $L1_2$-ordered phases in $Ni_3Al$ and $Cu_3Au$ were both calculated. Agreement with previous results was good for $Ni_3Al$, but there are still many unanswered questions concerning the experimental and theoretical work to date on the entropy difference; research is ongoing. Agreement with previous results was poor for $Cu_3Au$, and efforts at generating a more reliable potential are underway.

### Acknowledgment

The authors would like to thank C. Wolverton, M. Asta, S. Foiles, and A. Quong for helpful and stimulating discussions. Work was supported by the U.S. Department of Energy, Office of Basic Energy Sciences, Division of Materials Sciences under contract No. DE-AC04-94AL85000. Research by D. Morgan was also supported by the Director, Office of Energy Research, Office of Basic Energy Sciences, Division of Materials Sciences, of the U.S. Department of Energy under contract No. DE-AC03-76SF00098.

### Cited References

1. L. Anthony, J.K. Okamoto, and B. Fultz, *Phys. Rev. Lett., 70,* 1128 (1993).
2. B. Fultz, L. Anthony, L.J. Nagel, R.M. Nicklow, and S. Spooner, *Phys. Rev. B, 52,* 3315 (1995).
3. L.J. Nagel, L. Anthony, and B. Fultz, *Philos. Mag. Lett., 72,* 421 (1995).
4. F. Cleri and V. Rosato, *Philos. Mag. Lett., 67,* 369 (1993).
5. G.J. Ackland, *Alloy Modeling and Design,* G. Stocks and P. Turchi, Ed., The Minerals, Metals, and Materials Society, Warrendale, PA, 149 (1994).
6. J.D. Althoff, D. Morgan, D. de Fontaine, M. Asta, S.M. Foiles, and D.D. Johnson, *Phys. Rev. B, 56,* R5705 (1997).
7. R. Ravelo, J. Aguilar, M. Baskes, J.E. Angelo, B. Fultz, and B.L. Holian, *Phys. Rev. B, 57,* 862 (1998)
8. A. van de Walle and G. Ceder, *Phys. Rev. Lett., 80,* 4911 (1998)
9. M.S. Daw and M.I. Baskes, *Phys. Rev. B, 29,* 6443 (1984).
10. M.S. Daw, S.M. Foiles, and M.I. Baskes, *Mater. Sci. Rep., 9,* 251 (1993).
11. A.A. Maradudin, E.W. Montroll, G.H. Weiss, and I.P. Ipatova, *Theory of Lattice Dynamics in the Harmonic Approximation,* 2nd ed., Academic Press, New York (1971).
12. J. Callaway, *Quantum Theory of the Solid State,* Academic Press, San Diego, CA (1974).
13. J.M. Sanchez, F. Ducastelle, and D. Gratias, *Physica, 128A,* 334 (1984).
14. D. de Fontaine, *Solid State Phys., 47,* 33 (1994).
15. G.D. Garbulsky and G. Ceder, *Phys. Rev. B, 49,* 6327 (1994).

16. G.D. Garbulsky and G. Ceder, *Phys. Rev. B, 53,* 8993 (1996).
17. A. Zunger, S.-H. Wei, L.G. Ferreira, and J.E. Bernard, *Phys. Rev. Lett., 65,* 353 (1990).
18. K.C. Hass, L.C. Davis, and A. Zunger, *Phys. Rev. B, 42,* 3757 (1990).
19. S.-H. Wei, L.G. Ferreira, J.E. Bernard, and A. Zunger, *Phys. Rev. B, 42,* 9622 (1990).
20. A.F. Voter and S.P. Chen, *Mater. Res. Soc. Symp. Proc., 82,* 175 (1988).
21. S.M. Foiles, M.I. Baskes, and M.S. Daw, *Phys. Rev. B, 33,* 7983 (1986).
22. S.M. Foiles, *Phys. Rev. B, 49,* 14930 (1994).
23. G. Moraitis and F. Gautier, *J. Phys. F, 7,* 1421 (1977).
24. A. Zunger, *Statics and Dynamics of Alloy Phase Transformations,* P.E.A. Turchi and A. Gonis, Ed., Vol. 319, *NATO Advanced Study Institute, Series B: Physics,* Plenum, New York (1994).
25. J.W.D. Connolly and A.R. Williams, *Phys. Rev. B, 27,* 5169 (1983).
26. Z.W. Lu, S.-H. Wei, A. Zunger, S. Frota-Pessoa, and L.G. Ferreira, *Phys. Rev. B, 44,* 512 (1991).
27. M.D. Asta, Ph.D. dissertation, University of California at Berkeley (1993).
28. Obtained from C. Wolverton, personal communication.
29. D.D. Johnson, unpublished data.
30. C. Wolverton, unpublished data.
31. F. Cardellini, F. Cleri, G. Mazzone, A. Montone, and V. Rosato, *J. Mater. Res., 8,* 2504 (1993).